1-1-2009

Fragmentation Pathways of 2,3-dimethyl-2,3-dinitrobutane Cations in the Gas Phase

Martin Paine
University of Wollongong, mrlp93@uow.edu.au

Benjamin Kirk
University of Wollongong, bbk84@uow.edu.au

Simon Ellis-Steinborner
Defence Science and Technology Organisation

Stephen J. Blanksby
University of Wollongong, blanksby@uow.edu.au

Fragmentation Pathways of 2,3-dimethyl-2,3-dinitrobutane Cations in the Gas Phase

Abstract

2,3-Dimethyl-2,3-dinitrobutane (DMNB) is an explosive taggant added to plastic explosives during manufacture making them more susceptible to vapour-phase detection systems. In this study, the formation and detection of gas-phase [M+H](+), [M+Li](+), [M+NH4](+) and [M+Na](+) adducts of DMNB was achieved using electrospray ionisation on a triple quadrupole mass spectrometer. The [M+H](+) ion abundance was found to have a strong dependence on ion source temperature, decreasing markedly at source temperatures above 50 degrees C. In contrast, the [M+Na](+) ion demonstrated increasing ion abundance at source temperatures up to 105 degrees C. The relative susceptibility of DMNB adduct ions toward dissociation was investigated by collision-induced dissociation. Probable structures of product ions and mechanisms for unimolecular dissociation have been inferred based on fragmentation patterns from tandem mass (MS/MS) spectra of source-formed ions of normal and isotopically labelled DMNB, and quantum chemical calculations. Both thermal and collisional activation studies suggest that the [M+Na](+) adduct ions are significantly more stable toward dissociation than their protonated analogues and, as a consequence, the former provide attractive targets for detection by contemporary rapid screening methods such as desorption electrospray ionisation mass spectrometry. Copyright (C) 2009 Commonwealth of Australia. Published by John Wiley & Sons, Ltd.

Keywords

dimethyl, gas, 3, 2, pathways, fragmentation, cations, dinitrobutane, phase

Disciplines

Life Sciences | Physical Sciences and Mathematics | Social and Behavioral Sciences

RAPID COMMUNICATIONS IN MASS SPECTROMETRY
Rapid Commun. Mass Spectrom. 2009; **23**: 2867–2877
Published online in Wiley InterScience (www.interscience.wiley.com) DOI: 10.1002/rcm.4192

RCM

Fragmentation pathways of 2,3-dimethyl-2,3-dinitrobutane cations in the gas phase

Martin R. L. Paine[1], Benjamin B. Kirk[1], Simon Ellis-Steinborner[2]* and Stephen J. Blanksby[1]**

[1]School of Chemistry, University of Wollongong, Wollongong NSW, 2522, Australia
[2]Threat Mitigation Group, Weapon Systems Division, Defence Science and Technology Organisation, Edinburgh SA, 5111, Australia

Received 6 April 2009; Revised 1 July 2009; Accepted 5 July 2009

2,3-Dimethyl-2,3-dinitrobutane (DMNB) is an explosive taggant added to plastic explosives during manufacture making them more susceptible to vapour-phase detection systems. In this study, the formation and detection of gas-phase $[M+H]^+$, $[M+Li]^+$, $[M+NH_4]^+$ and $[M+Na]^+$ adducts of DMNB was achieved using electrospray ionisation on a triple quadrupole mass spectrometer. The $[M+H]^+$ ion abundance was found to have a strong dependence on ion source temperature, decreasing markedly at source temperatures above 50°C. In contrast, the $[M+Na]^+$ ion demonstrated increasing ion abundance at source temperatures up to 105°C. The relative susceptibility of DMNB adduct ions toward dissociation was investigated by collision-induced dissociation. Probable structures of product ions and mechanisms for unimolecular dissociation have been inferred based on fragmentation patterns from tandem mass (MS/MS) spectra of source-formed ions of normal and isotopically labelled DMNB, and quantum chemical calculations. Both thermal and collisional activation studies suggest that the $[M+Na]^+$ adduct ions are significantly more stable toward dissociation than their protonated analogues and, as a consequence, the former provide attractive targets for detection by contemporary rapid screening methods such as desorption electrospray ionisation mass spectrometry. Copyright © 2009 Commonwealth of Australia. Published by John Wiley & Sons, Ltd.

In 1991, the Marking of Plastic Explosives (MARPLEX) convention was adopted in Montreal, Canada, after a number of civilian aircraft were sabotaged in the late 1980s.[1] The MARPLEX convention aims to prevent terrorists (or for that matter any other person with no legitimate right to them) being able to obtain unmarked plastic explosives.[1] The convention also details the addition of 'odorants' or 'taggants', chemical components added to an explosive during manufacture to increase the overall vapour pressure of the product. The high vapour pressure of the odorant makes it susceptible to detection by commonly used vapour sampling methods and thus improves the likelihood of discovery of concealed explosives. Four odorants that were identified by the convention are 2,3-dimethyl-2,3-dinitrobutane (DMNB, Fig. 1(a)), ethylene glycol dinitrate (EGDN, Fig. 1(b)), *para*-mononitrotoluene (*p*-MNT, Fig. 1(c)) and *ortho*-mononitrotoluene (*o*-MNT, Fig. 1(d)).[2] DMNB was identified as the odorant of choice for marking plastic explosives as it is a white crystalline solid, has a relatively high vapour pressure (2.07×10^{-3} Torr at 25°C) compared with the plastic explosive 1,3,5-trinitro-1,3,5-triazacyclohexane (RDX) (1.4×10^{-9} Torr at 25°C, Fig. 1(e)), has no wide industrial usage, except as an additive in diesel fuel[3] and, as such, is unlikely to give rise to false positives.

There are a number of technologies that are used for the detection of explosives that may be suitable for the detection of taggants including ion mobility spectrometry (IMS),[2–4] solid-phase microextraction (SPME) gas chromatography,[5] capillary electrophoresis chromatography (CEC),[6] fluorescent detection (using zinc coordination compounds),[7,8] amplifying fluorescent polymer and organic nanofibril film sensors[9,10] and voltammetric sensing.[11] IMS is one of the most commonly used techniques for explosive detection, typically employing temperatures above 100°C to volatilise these compounds. It has been shown, however, that in positive ion mode, detection of the taggant DMNB by IMS can be significantly diminished at these operating temperatures.[12] This is demonstrated in Fig. 2 where the clear DMNB signal in the low-temperature plasmogram (40°C) is markedly diminished even at 81°C where a concomitant rise in other ion signals is observed.[12] It has been suggested that this effect is due to thermal decomposition and/or ion-molecule reactions of either neutral or ionised DMNB.[1–4,13–15] The structures of ions resulting from either of these processes have yet to be experimentally characterised and the suggested pathways for their formation have only been inferred from the solution-phase chemistry of nitroalkanes.

**Correspondence to*: S. Ellis-Steinborner, Threat Mitigation Group, Weapon Systems Division, Defence Science and Technology Organisation, P.O. Box 1500 Edinburgh, S.A., 5111, Australia.
E-mail: simon.ellis-steinborner@dsto.defence.gov.au
***Correspondence to*: S. J. Blanksby, School of Chemistry, University of Wollongong, Wollongong, New South Wales, 2522, Australia.
E-mail: blanksby@uow.edu.au

RCM

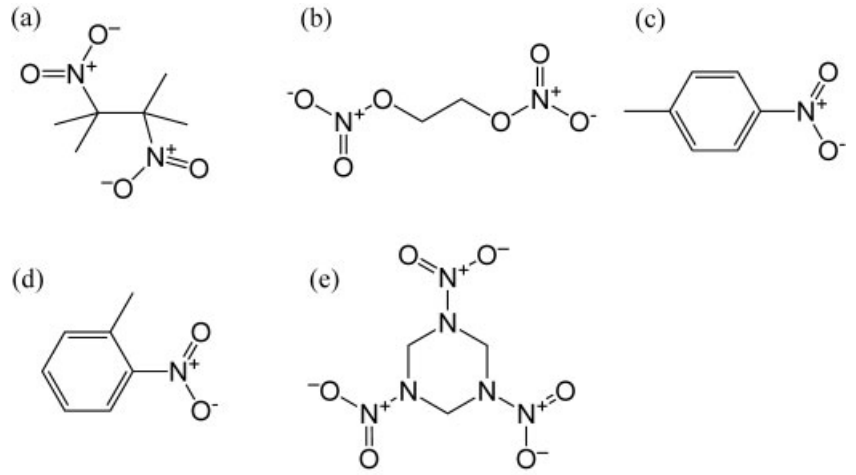

Figure 1. Molecular structures of (a) DMNB, (b) EGDN, (c) *p*-MNT, (d) *o*-MNT, and (e) RDX.

In the present study four positively charged DMNB adduct ions, namely, $[M+H]^+$, $[M+Li]^+$, $[M+NH_4]^+$ and $[M+Na]^+$, have been generated using positive ion electrospray ionisation (ESI) tandem mass spectrometry (MS/MS) in a triple quadrupole instrument. The stability of these ions with respect to thermal and collisional decomposition has been investigated. Collision-induced dissociation (CID) spectra from ionised DMNB and its isotopologue D_{12}-DMNB are presented and provide for the identification of product ions, as well as potential mechanisms for unimolecular decomposition. These data may provide insight into the pathways of thermal decomposition of ionised DMNB species within an IMS explosive detection device at common operating temperatures.

EXPERIMENTAL

Electrospray ionisation mass spectrometry

2,3-Dimethyl-2,3-dinitrobutane was purchased from Sigma-Aldrich (Seven Hills, NSW, Australia) and was used without further purification. Deuterated DMNB (D_{12}-2,3-dimethyl-2,3-dinitrobutane) was purchased through Sigma-Aldrich (Seven Hills, NSW, Australia), having been synthesised by ISOTEC (Miamisburg, OH, USA) to a purity of 97%, and was used without further purification. Methanol, chloroform and formic acid were HPLC grade (Crown Scientific, Minto, NSW, Australia). Lithium acetate, ammonium acetate and sodium chloride were obtained from Sigma-Aldrich (Castle Hill, NSW, Australia). Mass spectra were obtained using a QuattroMicro triple quadrupole mass spectrometer (Waters, Manchester, UK). Standard solutions of DMNB (40 μM) were prepared in methanol with the appropriate dopants added as indicated to final concentrations of: formic acid (1% v/v), lithium acetate (0.05% w/v) ammonium acetate (40 μM) and sodium chloride (0.05% w/v). Spectra were obtained by infusion of standard solutions (10 $\mu L\,min^{-1}$) with the following conditions applied to the instrument: capillary voltage 3.8 kV, cone voltage 25 V, source temperature 120°C (unless otherwise indicated). Argon was used as the collision gas at a pressure of 4×10^{-3} Torr. The mass resolution for ESI-MS and ESI-MS/MS experiments was typically 0.75 *m/z* units across the entire mass range and all spectral data presented result from the average of at least 200 scans. The data were baseline-subtracted (40% background subtract

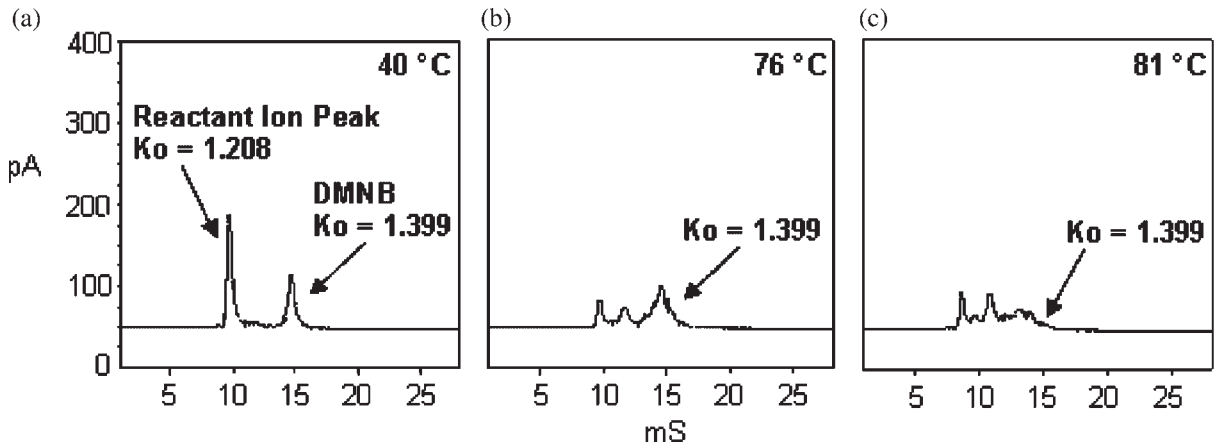

Figure 2. The positive ion IMS plasmograms of DMNB with a reduced mobility (Ko) of 1.399 with the membrane and drift tube temperatures at (a) 40°C and 44.8°C, respectively; (b) 76°C and 34°C, respectively; and (c) 81°C and 76°C, respectively.

DOI: 10.1002/rcm

with a first-order polynomial) and smoothed (two mean smooths using a peak width of 0.75 *m/z* units) using the MassLynx software (Water).

Desorption electrospray ionisation mass spectrometry

A methanolic solution of DMNB (1 mg mL^{-1}) doped with NaCl (0.05% w/v) was deposited at ca. 50 ng cm^{-2} on an Omni Slide™ hydrophobic array (Prosolia Inc., Indianapolis, IN, USA) and allowed to dry prior to analysis. Desorption electrospray ionisation (DESI) mass spectra were obtained using an LTQ linear ion trap mass spectrometer (Thermo-Finnnigan, San Jose, CA, USA) equipped with an Omni Spray™ DESI source (Prosolia Inc.). The source was operated in positive ion mode using methanol as the spray solvent (3 μL min^{-1}) and nitrogen as the nebulising gas (backing pressure of 80 psi). The spray voltage was typically 4 kV with the emitter positioned 5 mm from the sample and 2 mm from the inlet to the mass spectrometer. An incident angle (α) of 55° and a collection angle (β) of 15–20° were employed. The heated inlet capillary was set to 150°C. For CID experiments an isolation width of 2 *m/z* units was used with an activation energy set to 25 arbitrary units and an activation time of 30 ms. Spectra represent an average of at least 50 scans combined using the Xcalibr 2.0 software (ThermoFinnnigan).

Electronic structure calculations

Geometry optimisations were carried out with the B3LYP method using the 6-311++G(d,p) basis set within the Gaussian03 suite of programs[16] which specifies tight convergence criteria by default (SCF = TIGHT) for this approach. Frequency calculations provided zero-point energies, which were used – without empirical scaling factors – to correct the calculated electronic energy. Full geometries of all optimised stationary points are provided as Supporting Information.

RESULTS AND DISCUSSION

ESI mass spectra of methanolic solutions of DMNB were recorded in the presence of formic acid, lithium acetate, ammonium acetate and sodium chloride. Representative spectra obtained under these conditions are presented in Fig. 3. Interestingly, a prominent $[DMNB+Na]^+$ adduct ion at *m/z* 199 appears not only in Fig. 3(d), where sodium chloride has been added, but in all four mass spectra. In the spectra shown in Figs. 3(a)–3(c) no sodium has been deliberately added to the electrospray solution. The formation of such abundant sodium adducts in the presence of only trace amounts of sodium (presumably from glass) suggests a very high affinity of DMNB for this metal ion. Figures 3(a)–3(c) indicate the generation of the $[DMNB+H]^+$, $[DMNB+Li]^+$ and $[DMNB+NH_4]^+$ ions at *m/z* 177, 183 and 194, respectively. The $[DMNB+H]^+$ ion at *m/z* 177 (Fig. 3(a)) was exceedingly difficult to generate and could only be observed in the presence of a high concentration of formic acid (1% v/v) with the ESI source block and nebulising gas temperatures lowered to ca. 50°C from the standard operating temperature of 120°C.

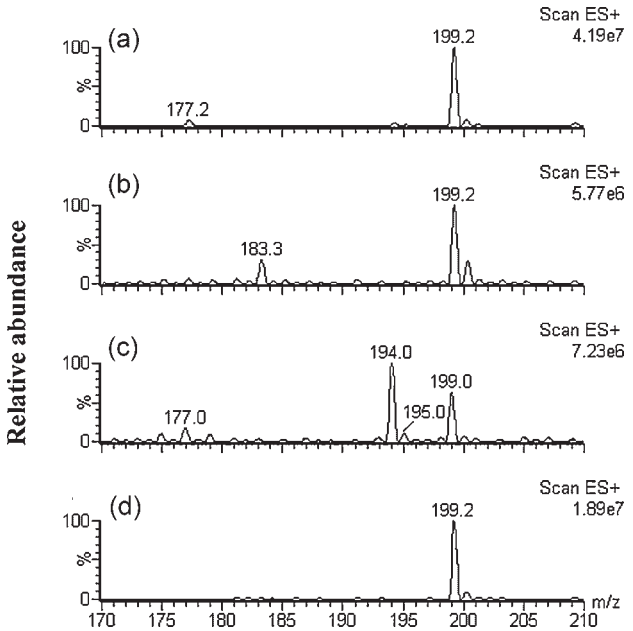

Figure 3. Positive ion ESI-MS spectra of methanolic solution of DMNB in the presence of: (a) formic acid, (b) lithium acetate, (c) ammonium acetate, and (d) sodium chloride on the triple quadrupole mass spectrometer at source temperature 40°C.

The observation of a temperature dependence of the $[DMNB+H]^+$ ion is consistent with the response of DMNB in IMS as noted earlier and this finding was thus systematically investigated.[14] The temperature profiles of the $[DMNB+H]^+$, $[DMNB+NH_4]^+$ and $[DMNB+Na]^+$ ion current were acquired and compared with the total ion current (TIC) generated by ESI-MS of the solution. This was achieved by incrementally raising both the desolvation gas and ESI source block temperatures at 2.5°C min^{-1} over the range of 25–105°C while continuously obtaining mass spectra over the desired mass range. From these data, the ion currents at *m/z* 177 ($[DMNB+H]^+$), 194 ($[DMNB+NH_4]^+$) and 199 ($[DMNB+Na]^+$) were extracted and compared with the TIC, as shown in Fig. 4. The TIC increases steadily over the entire temperature range, which is consistent with an overall increase in ion formation due to more efficient desolvation at higher temperatures.[17] This trend is also observed in the extracted chromatogram of $[DMNB+Na]^+$ but, in contrast, the *m/z* 177 ion current corresponding to protonated DMNB exhibits a maximum abundance at ca. 50°C followed by a decrease at higher temperatures. A similar steady decrease of ion current is observed at temperatures above 50°C for the *m/z* 194 ion ($[DMNB+NH_4]^+$). This would suggest that the thermal stability of DMNB, as observed in IMS, may be dependent on the type of adduct formed. This dependency could therefore be exploited to obtain an increase in ion stability and thus improved detection sensitivity. Given the complexity of the ESI-MS spectra obtained it was not possible to readily identify the rise of ionic products that may correlate with the diminishing $[M+H]^+$ signal at higher temperatures. Thus, CID experiments were carried out to determine the potential identity of product ions arising in ESI-MS and IMS analysis.

DOI: 10.1002/rcm

RCM

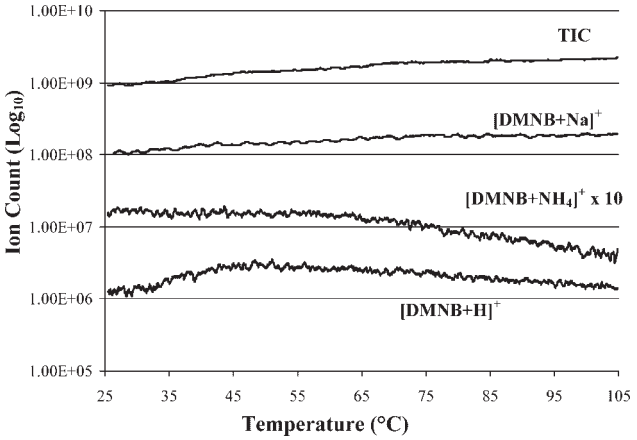

Figure 4. A graph of the ion count produced by ESI at varying source temperatures (°C) for ions at m/z 177 $[DMNB+H]^+$, 194 $[DMNB+NH_4]^+$, 199 $[DMNB+Na]^+$, and the total ion current (TIC).

CID of $[DMNB+H]^+$

The positive ion ESI-MS/MS product ion spectra for the $[DMNB+H]^+$, $[DMNB+Li]^+$ and $[DMNB+Na]^+$ ions were recorded using the triple quadrupole mass spectrometer and the spectra are presented in Fig. 5. At laboratory collision energies as low as 1 eV the ion at *m/z* 177 corresponding to the $[DMNB+H]^+$ ion shows extensive fragmentation with the product ion at *m/z* 130 having a relative abundance of 90% of the precursor ion (Fig. 6). This represents significant decomposition of the precursor ion at centre-of-mass energies E_{CM} <20 kJ mol^{-1} (calculated for the laboratory-frame energy $E_{LAB} = 1$ eV with argon as the collision partner).[18] Considering that covalent bonds typically require more than 10 times this amount of energy for dissociation (i.e., a typical carbon–carbon single bond energy is ~360 kJ mol^{-1}),[19] it is apparent that the $[DMNB+H]^+$ ion is exceptionally fragile. As the laboratory-frame collision energy increases to 5 eV (E_{CM} ~90 kJ mol^{-1}) the relative abundance of the ion at *m/z* 177 decreases to 30% of the base peak.

Closer examination of the ESI-MS/MS spectra in the inset in Fig. 6 also reveals a product ion at *m/z* 195. This ion corresponds to the addition of a nominal mass of 18 *m/z* units to the precursor ion, which can be attributed to the addition of water. As the background concentration of water in the analyser portion of the instrument is expected to be low, this suggests a very efficient adduct-forming reaction between the $[DMNB+H]^+$ ion and water. The reactivity of this ion towards water is particularly problematic for IMS analysis, which often utilises air as a carrier gas for the introduction of

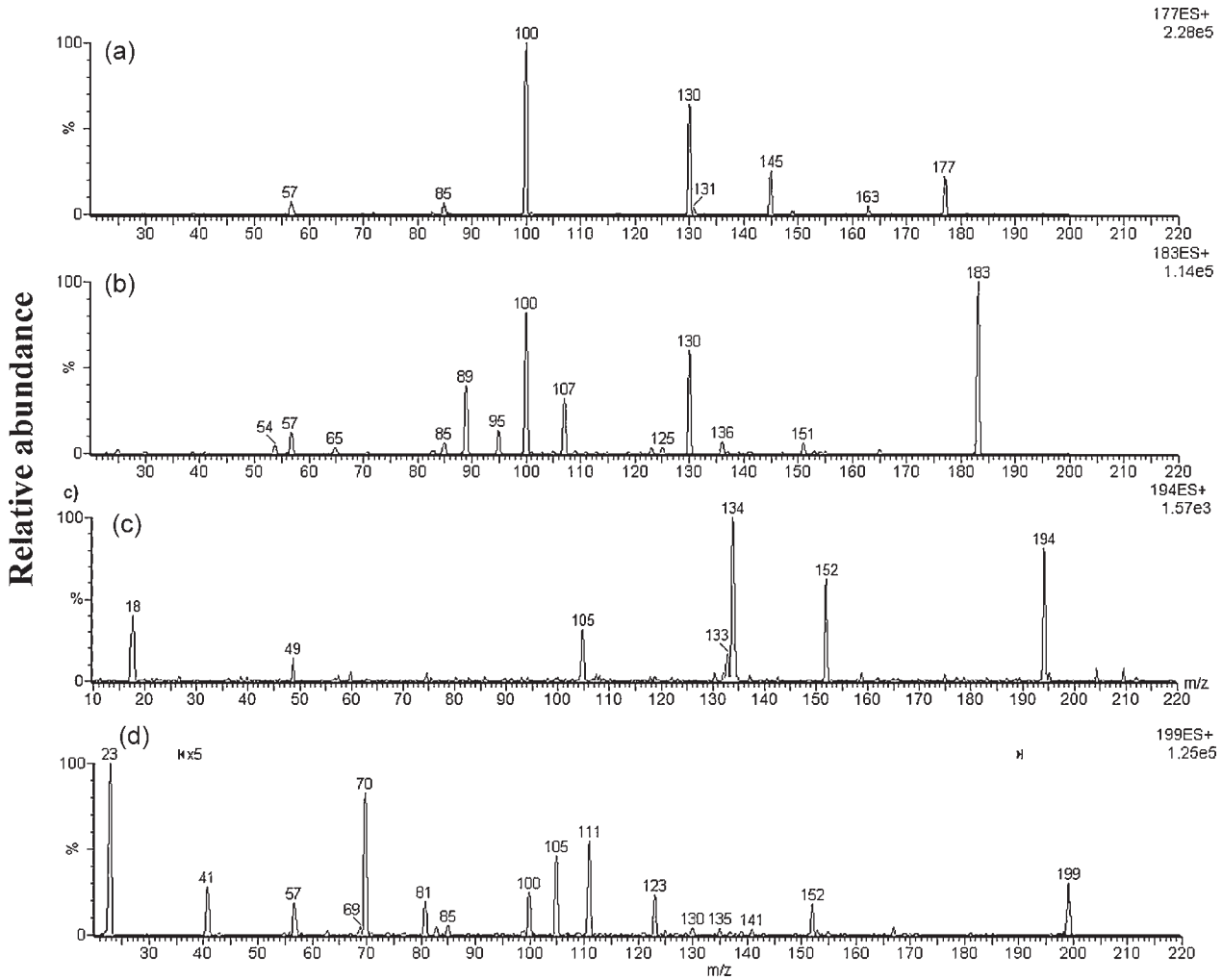

Figure 5. Positive ion ESI-MS/MS spectra of: (a) $[DMNB+H]^+$ *m/z* 177 ($E_{LAB} = 5$ eV), (b) $[DMNB+Li]^+$ *m/z* 183 ($E_{LAB} = 15$ eV), (c) $[DMNB+NH_4]^+$ *m/z* 194 ($E_{LAB} = 10$ eV), and (d) $[DMNB+Na]^+$ *m/z* 199 ($E_{LAB} = 15$ eV) on the triple quadrupole mass spectrometer at the ESI source temperature of 50°C.

DOI: 10.1002/rcm

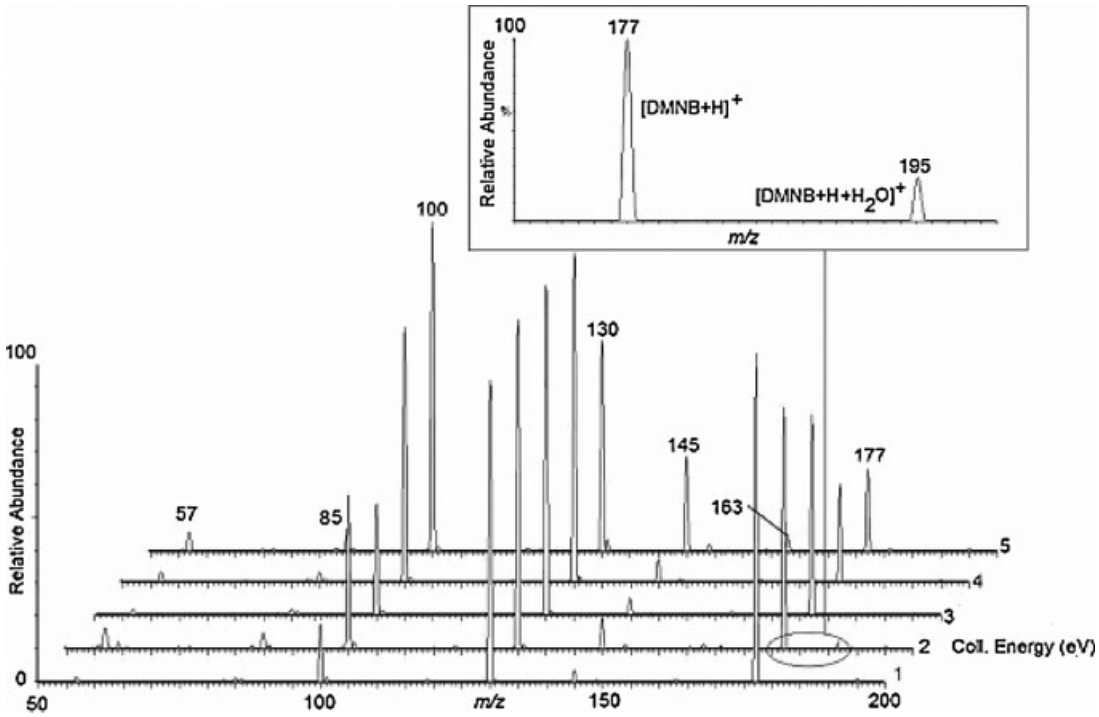

Figure 6. Positive ion ESI-MS/MS spectra of $[DMNB+H]^+$ (*m/z* 177) at 40 °C with CID at collision energies $E_{LAB} = 1–5$ eV. Inset: region of spectrum magnified to show the addition of H_2O (18 Da) to $[DMNB+H]^+$ to yield the ion at *m/z* 195.

analytes into the ionisation cell. Under these conditions the analogous addition of water is expected to be even more facile, thus resulting in peak broadening and decreased detection efficiency within the ion mobility spectrometer.[3,14]

The major product ions observed from CID of $[DMNB+H]^+$ (Fig. 5(a)) are at *m/z* 145, 130, 100 and 85. Secondary fragmentation of each of these product ions was achieved by adjusting the cone voltage to maximise fragmentation of the precursor ions during extraction from the ESI source. This was followed by recording CID spectra of the source-formed product ions which, henceforth, will be referred to as pseudo-MS^3 data (Table 1). The product ion at *m/z* 145 corresponds to a loss of a nominal mass of 32 Da from the precursor cation and can be attributed to the loss of either methanol (CH_3OH) and/or dioxygen (O_2). The ESI-MS/MS spectrum of D_{12}-DMNB was obtained under identical conditions and shows exclusive loss of 32 Da (Table 1), confirming the loss of dioxygen. The proposed mechanism for O_2 loss (Scheme 1) involves peroxide bond formation followed by condensation of the intermediate peroxide ring via either nitrogen–nitrogen or nitrogen–oxygen bond formation leading to the neutral loss of O_2 with the formation of 2-hydroxy-3,3,4,4-tetramethyl-1-oxo-1,2-diazetidin-1-ium (Scheme 1(a)) and/or 3,3,4,4-tetramethyl-2-oxo-1,2,5-oxadiazolidin-2-ium cations (Scheme 1(b)). Further fragmentation of the product ion at *m/z* 145 yields *m/z* 85 (Table 1)

Table 1. Collision-induced dissociation mass spectra of ionised DMNB and source-formed product ions recorded on an ESI triple quadrupole mass spectrometer. The mass-to-charge ratio of the precursor ion is underlined in the peak list

Precursor ion	E_{LAB} (eV)	Product ions *m/z* (% abundance)
$[DMNB+H]^+$	<1	195(3), 177(100), 163(5), 145(35), 130(60) 100(45), 85(10), 57(10)
$[D_{12}$-DMNB+H$]^+$	<1	189(55), 157(1), 142(100), 112(50), 94(5), 66(15)
*$[DMNB+H-14]^+$	<1	163(100), 145(4), 85(3)
*$[DMNB+H-32]^+$	<1	163(3), 145(100), 85(6)
*$[DMNB+H-47]^+$	<1	130(100), 100(30), 85(3), 57(6)
*$[DMNB+H-77]^+$	<1	100(100), 85(40), 57(80)
*$[[DMNB+H-92]^+$	<1	85(100), 57(10)
*$[[DMNB+H-120]^+$	15	57(100), 41(31), 39(35)
$[DMNB+Li]^+$	10	183(100), 151(6), 136(7), 130(65), 107(36), 100(93), 95(13), 89(49), 85(8), 57(14), 54(5)
$[DMNB+^6Li]^+$	10	182(100), 150(6), 135(6), 130(69), 106(39), 100(87), 94(16), 88(65), 85(6), 57(22), 53(4)
$[D_{12}$-DMNB+Li$]^+$	10	195(54), 147(4), 142(68), 137(9), 119(35), 112(100), 101(17), 99(31), 94(10), 71(5), 66(27)
$[DMNB+Na]^+$	15	199(28), 152(3), 123(4), 111(9), 105(9), 100(4), 81(4), 70(17), 57(4), 41(6), 23(100)
$[D_{12}$-DMNB +Na$]^+$	15	211(18), 163(2), 135(5), 117(12), 115(4), 112(4), 87(2), 71(11), 66(8), 41(8), 23(100)
$[DMNB+ND_4]^+$	15	198(10), 22(100)

* Denotes source-formed precursor ions providing pseudo-MS^3 spectra.

DOI: 10.1002/rcm

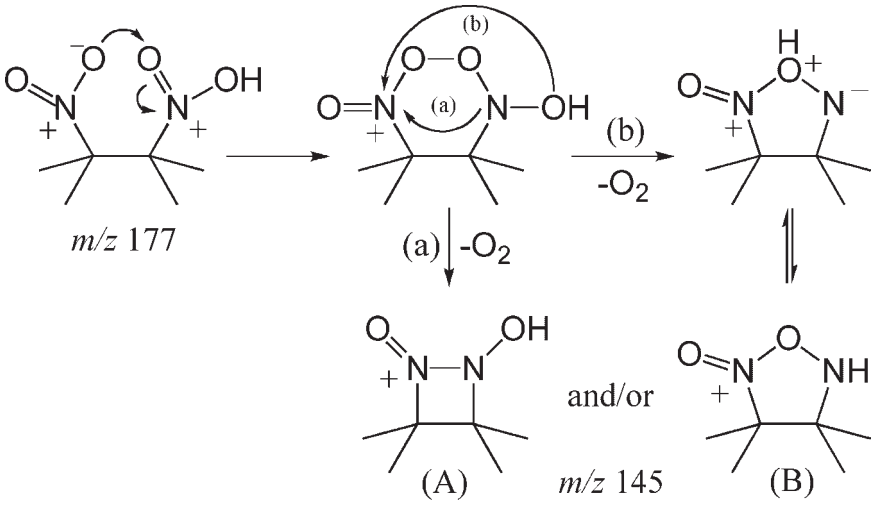

Scheme 1. Proposed fragmentation pathways for O_2 loss from $[DMNB+H]^+$.

corresponding to the consecutive loss of two molecules of nitric oxide (60 Da). This fragmentation is not sufficiently characteristic to discount either product ion structure but it is interesting to note that DMNB is used as a starting reagent in the synthesis of 3,3,4,4-tetramethyl-1,2-diazetine-1,2-dioxide.[20] This compound is a neutral analogue of product A from Scheme 1 and this perhaps suggests that this is the more probable structure for the *m/z* 145 ion.

Figure 6 also reveals an abundant product ion at *m/z* 130 corresponding to a neutral loss of 47 Da, which is attributed to extrusion of nitrous acid (HONO). This observation is consistent with the reported gas-phase fragmentation of other ionised nitroalkanes,[3,14,21] as well as the solution-phase thermolysis of vicinal dinitroalkanes.[22] The mechanism proposed for the loss of nitrous acid involves the concerted elimination of HONO to form protonated 2,3-dimethyl-2-nitrobut-3-ene (Scheme 2) and it is supported by the D_{12}-DMNB spectrum that shows the exclusive loss of HONO (Table 1).

The product ion at *m/z* 100 corresponds to a loss of nominal mass of 30 Da from the ion at *m/z* 130 and can be attributed to the loss of nitric oxide (NO). This sequential fragmentation mechanism is supported by the pseudo-MS^3 spectrum of *m/z* 130 that shows *m/z* 100 as a major product ion (Table 1). Loss of NO from a nitro-substituted compound must necessarily be preceded by unimolecular rearrangement to a nitrite ester. Two potential isomerisation mechanisms have been identified. In the first mechanism, the protonated nitro moiety attacks the terminal alkene position via a five-membered transition state (Scheme 3(a)), while, in the alternative pathway, an *ipso*-rearrangement yields a nitrite ester (Scheme 3(b)). In both instances the nascent esters can undergo homolytic cleavage of the N−O bond to yield nitric oxide and isomeric 2- and 3-butenol radical cations, respectively, at *m/z* 100. The pseudo-MS^3 spectrum of this product ion shows a loss of 15 Da (Table 1), which is consistent with loss of a methyl group to give the product ion at *m/z* 85, as indicated in Scheme 3(b). While this observation favours the latter mechanism, it would be difficult to unequivocally distinguish these two pathways and indeed both butenol isomers (Schemes 3(a) and 3(b)) may contribute to the ion population at *m/z* 100.

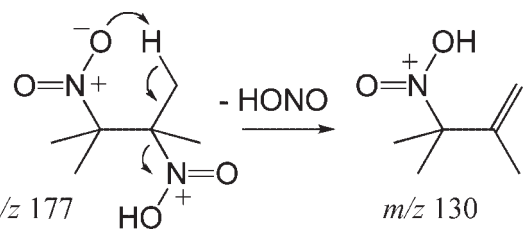

Scheme 2. Proposed fragmentation pathway for nitrous acid (HONO) loss from $[DMNB+H]^+$.

CID of $[DMNB+Li]^+$ and $[DMNB+Na]^+$

The CID spectra of the metal adducts, $[DMNB+Li]^+$ and $[DMNB+Na]^+$ (Figs. 5(b) and 5(c)), reveal several product ions that are directly analogous to those of the $[DMNB+H]^+$ ion discussed above (Fig. 5(a)). For example, the product ions at *m/z* 130, 100, 85 and 57 are common to all three ESI-MS/MS spectra in Fig. 5 and can be rationalised via fragmentation mechanisms similar to those postulated for protonated DMNB (cf. Schemes 1–3).

While the neutral losses of $LiNO_2$ and $NaNO_2$ (to yield *m/z* 130 in Figs. 5(b) and 5(c), respectively) can be rationalised by the mechanism in Scheme 2, the loss of HNO_2 from these metal adducts (to yield *m/z* 136 and 152, respectively) must necessarily occur by a different pathway. Elimination of nitrous acid via a five-membered transition state as indicated in Scheme 4 might be favoured in the presence of a metal ion. This process could also give rise to a second consecutive loss of HNO_2 to yield the metal adduct ions of 2,3-dimethylbutadiene observed at *m/z* 89 and 105 in Figs. 5(b) and 5(c), respectively. The elimination mechanism outlined in Scheme 4 can also give rise to the metal adduct ions of nitrous acid observed at *m/z* 54 for $[HONO+Li]^+$ and *m/z* 70 for $[HONO+Na]^+$. These ions could conceivably be formed at either of the elimination steps via neutral loss of 2,3-dimethyl-2-nitrobut-3-ene (Scheme 4(a)) or 2,3-dimethylbutadiene (Scheme 4(b)). The latter would seem more likely, given the expected higher metal ion affinity of the nitrous

DOI: 10.1002/rcm

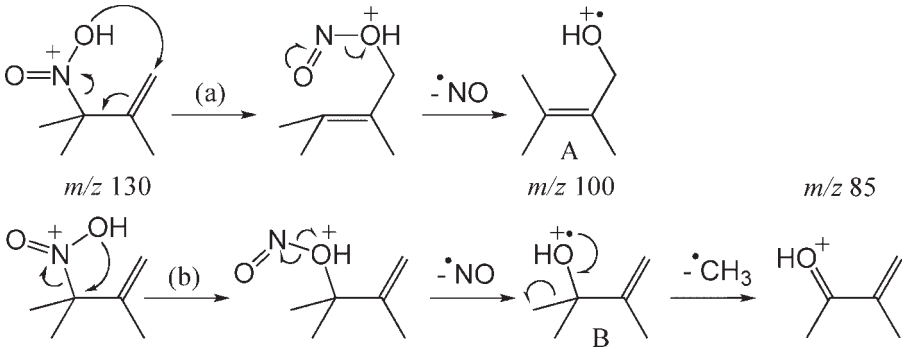

Scheme 3. Proposed unimolecular rearrangement and fragmentation of protonated 2,3-dimethyl-2-nitrobut-3ene.

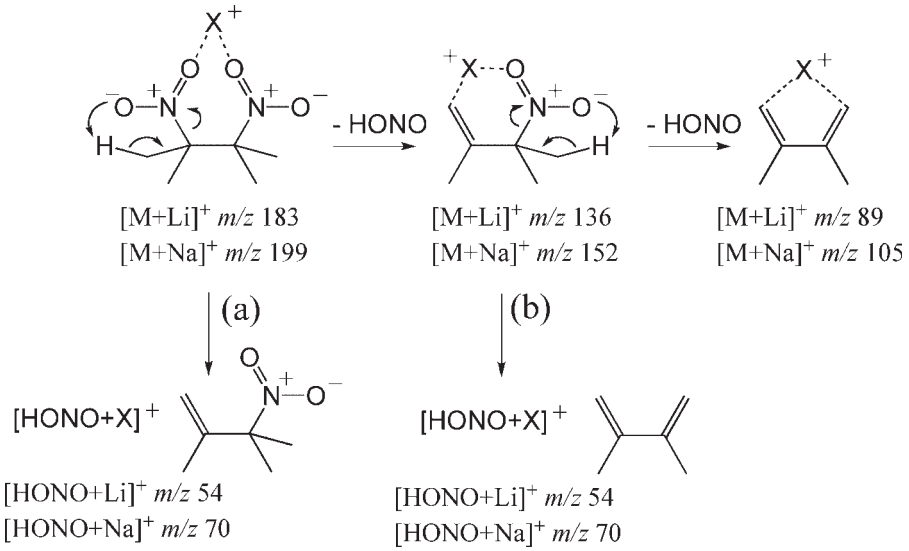

Scheme 4. Proposed fragmentation pathways for nitrous acid (HONO) loss from $[DMNB+Li]^+$ and $[DMNB+Na]^+$.

acid than of the butadiene. The sequential loss of nitrous acid observed in these CID spectra is analogous to that postulated by Munro *et al*. based on IMS-MS observations.[14]

CID of the $[M+Li]^+$ adduct ions give rise to abundant products at *m/z* 95 and 107, corresponding to neutral losses of 88 and 76 Da, respectively (Fig. 5(b)). The presence of lithium in these product ions was confirmed by the observation of ions at *m/z* 94 and 106 in the CID spectrum of the $[M+^6Li]^+$ cation at *m/z* 182 (Table 1). Neither the product ions nor the equivalent neutral losses are observed in the $[M+H]^+$ spectrum (Fig. 5(a)) but the analogous neutral losses are present in the CID spectrum of $[M+Na]^+$ (Fig. 5(c)) suggesting that this pathway is common to the metal adducts. These neutral losses are consistent with the empirical formulae N_2O_3 (76 Da) and $C_3H_6NO_2$ (88 Da) and such assignments are supported by the observation of neutral losses of 76 and 94 Da in the CID spectra of both [D_{12}-DMNB+Li]$^+$ and [D_{12}-DMNB+Na]$^+$ (Table 1). This fragmentation can be rationalised via an initial rearrangement of a nitro moiety to a nitrite ester followed by homolytic bond cleavage and loss of NO (Scheme 5). While the intermediate radical cation proposed in Scheme 5 is not observed experimentally, this nascent alkoxyl radical would be expected to undergo facile dissociation leading to competitive losses of NO_2 and CH_3COCH_3 (Scheme 5).

CID of $[DMNB+NH_4]^+$

The CID spectrum of the ammonium adduct, $[DMNB+NH_4]^+$ is shown in Fig. 5(d). The base peak in this spectrum is observed at *m/z* 134 resulting from a neutral loss of 60 Da corresponding to the empirical formula N_2O_2. This suggests a mechanism not dissimilar to that of the metallated cations shown in Scheme 5. In the case of the ammonium adduct, however, both nitro moieties undergo rearrangement to nitrite esters which both undergo ammonium-assisted dissociation to liberate two molecules of nitric oxide (Scheme 6(a)). A plausible competitive mechanism is shown in Scheme 6(b), whereby the ammonium protonates the DMNB on one of the nitro groups releasing ammonia within the product complex. The ammonia is sufficiently basic to effect facile elimination of the enol tautomer of 2-nitropropane and give rise to the ammonium adduct of 2-nitropropene at *m/z* 105. The product ion at *m/z* 152 probably arises from water addition to *m/z* 134. The CID spectrum of isotopically labelled $[DMNB+ND_4]^+$ was obtained (Table 1) in an effort to verify the role of proton transfer in this process. Unfortunately, this spectrum is dominated by the ND_4^+ product ion (*m/z* 22) arising from direct dissociation of the complex. This is presumably a result of weakened hydrogen bonding in the D_4-isotopologue. There is thus no direct experimental evidence for the putative mechanism shown.

DOI: 10.1002/rcm

RCM

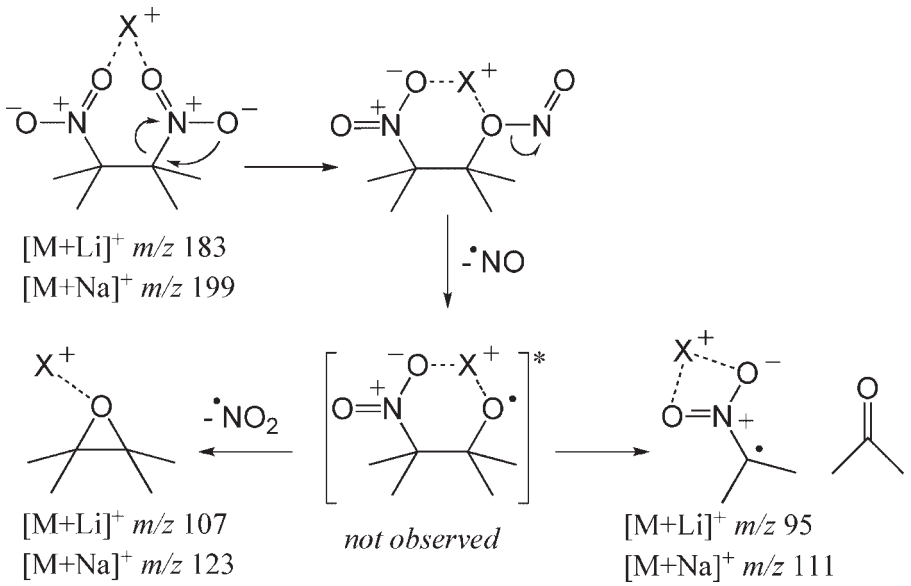

Scheme 5. Competitive fragmentation pathways proposed for $[DMNB+Li]^+$ and $[DMNB+Na]^+$ initiated by loss of a nitric oxide radical.

Comparison of relative stability of DMNB cations

In an effort to compare the relative stability of the adduct cations, the degree of fragmentation of each of these ions at the same laboratory frame collision energies was compared. Given the small mass differences between the four ions, the CID spectra recorded at a laboratory-frame collision energy of 10 eV yield centre-of-mass collision energies within a narrow range ($E_{CM} = 174–161$ kJ mol^{-1}). The precursor ion abundance from these data, expressed as a percentage of total ion count, was found to be 1, 23, 25 and 74% for $[DMNB+H]^+$, $[DMNB+Li]^+$, $[DMNB+NH_4]^+$ and $[DMNB+Na]^+$, respectively. This suggests that the ammonium and the metal adduct ions are significantly more stable with respect to dissociation than is the $[DMNB+H]^+$ ion. $[DMNB+Na]^+$ in particular exhibits fewer product ions arising from decomposition of the DMNB molecule, favouring instead the formation of free Na^+ ions (*m/z* 23) as the major dissociation pathway (Fig. 5(d)). These observations suggest that ammonium and metal ion adducts of DMNB may represent a more robust target for detection in analytical protocols (see later) but raise the interesting question as to the source of this additional stability.

Electronic structure calculations of protonated and sodiated DMNB

Electronic structure calculations of neutral DMNB along with its $[DMNB+H]^+$ and $[DMNB+Na]^+$ analogues have been performed at the B3LYP/6-311++G(d,p) level of theory. The optimised structures for both *syn*- and *anti*-conformations are provided in Fig. 7 and the electronic energies for all the structures are listed in Table 2. Full structural definitions of all stationary point geometries are provided as Supporting Information. Not surprisingly, while the *anti*-conformation is the global minimum for neutral DMNB, for the ionised forms the *syn*-configuration (where the proton or sodium ion interact simultaneously with both nitro groups) was found to

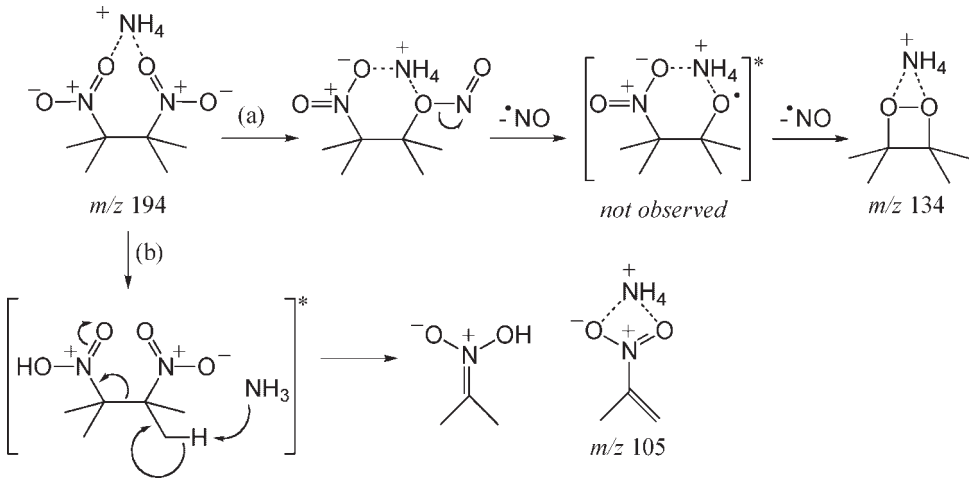

Scheme 6. Proposed fragmentation pathways for $[DMNB+NH_4]^+$.

DOI: 10.1002/rcm

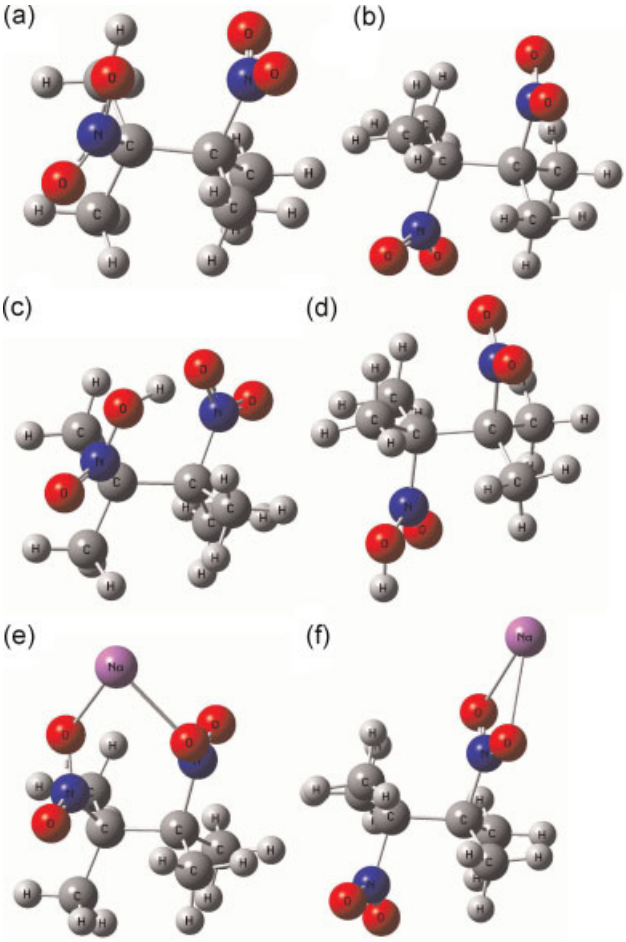

Figure 7. Molecular geometries optimised at the B3LYP/6-311++G(d,p) level of theory for (a) *syn*-DMNB, (b) *anti*-DMNB, (c) *syn*-$[DMNB+H]^+$, (d) *anti*-$[DMNB+H]^+$, (e) *syn*-$[DMNB+Na]^+$, and (f) *anti*-$[DMNB+Na]^+$. The electronic and zero-point energies of each of these structures are provided in Table 2.

be lower in energy by 51.5 and 43.4 kJ mol^{-1} for the $[DMNB+H]^+$ and $[DMNB+Na]^+$ ions, respectively (Table 2).

Two mechanisms for the decomposition of ionised DMNB were proposed and are outlined in Scheme 7. Charge-remote elimination of HONO from cationised DMNB (Scheme 7(a)) may proceed from the *anti*-conformation of both $[DMNB+H]^+$ and $[DMNB+Na]^+$ via structurally similar transition states. The preference for the *anti*-configuration presumably arises from the increased basicity of the nitro moiety in the absence of any direct association with the cation. While the pathway in Scheme 7(a) is calculated to be only slightly endothermic for both cations, a significant thermodynamic barrier to decomposition was identified, with activation energies of 177.9 and 178.2 kJ mol^{-1} for $[DMNB+H]^+$ and $[DMNB+Na]^+$, respectively. This suggests that the charge-remote elimination pathway cannot account for the observed low-energy decomposition of $[DMNB+H]^+$ which was shown to be facile even at very low collision energies. In contrast, this pathway could reasonably account for the observation of nitrous acid loss at low abundance in the CID spectrum of $[DMNB+Na]^+$ (i.e. to form the product ion of *m/z* 152 in Fig. 5(d)).

Initial investigations of an alternative pathway for decomposition focused on the putative mechanism outlined in Scheme 2 whereby the uncharged nitro moiety acts as a base to abstract a γ-hydrogen and eliminate the nitro group and the charge carrier. While no transition states for this E2 reaction were located for the $[DMNB+H]^+$ system, a transition state was identified for an intramolecular substitution pathway. This process also proceeds from the *anti*-conformer where C–N bond heterolysis yields an intermediate carbocation complex that undergoes subsequent ring closure initiated by the remaining nitro moiety (Scheme 7(b)). The calculated activation barrier for this intramolecular S_N1 process is just 55.0 kJ mol^{-1} with respect to the *syn*-conformation of $[DMNB+H]^+$. The reaction yields a cyclic 2-oxo-1,2-oxaazetidinium cation (Scheme 7(b)) that was found to be some 38.3 kJ mol^{-1} more stable than the isomeric alkene formed via the elimination mechanism in Scheme 7(a). Significantly, these data suggest that if the cation arises from protonation of the *anti*-conformation of neutral DMNB (the lower energy conformation on the neutral potential energy surface), decomposition will be *exothermic* by 49.9 kJ mol^{-1} over an activation barrier of just 3.5 kJ mol^{-1}. This very low dissociation energy is consistent with the experimental observation of facile loss of nitrous acid from the $[M+H]^+$ ion at activation energies estimated to be as low as 20 kJ mol^{-1} (*vide supra*). Furthermore, the possibility of near direct dissociation upon protonation of the *anti*-conformation of DMNB may contribute to the difficulties

Table 2. Electronic and zero-point energies for conformers of DMNB, $[DMNB+H]^+$ and $[DMNB+Na]^+$ ions calculated at the B3LYP/6-311++G(d,p) level of theory using the Gaussian03 suite of programs. Optimised structures for each of these molecules are shown in Fig. 7

Molecule or ion	Conformer	Energy (Hartrees)	Zero-point energy (Hartrees)	Energy + ZPE (Hartrees)	Relative energy (kJ mol^{-1})
DMNB	*syn*	−646.26977	0.19448	−646.07529	—
	anti	−646.27323	0.19456	−646.07866	—
$[DMNB+H]^+$	*syn*	−646.58815	0.20436	−646.38379	0.0
	anti	−646.57008	0.20536	−646.36472	+51.5
$[DMNB+Na]^+$	*syn*	−808.42154	0.19567	−808.22587	0.0
	anti	−808.40470	0.19524	−808.20946	+43.4
*$[TS7(a)+H]^+$		−646.51459	0.19605	−646.31854 (−1456 cm^{-1})	+177.9
		−646.56480	0.19947	−646.36534 (−66 cm^{-1})	+55.0
*$[TS7(a)+Na]^+$		−808.34626	0.18611	−808.16015 (−1403 cm^{-1})	+178.2

* $[TS7(a)+H]^+$ refers to the transition state for the mechanism of dissociation outlined in Scheme 7(a).

DOI: 10.1002/rcm

RCM

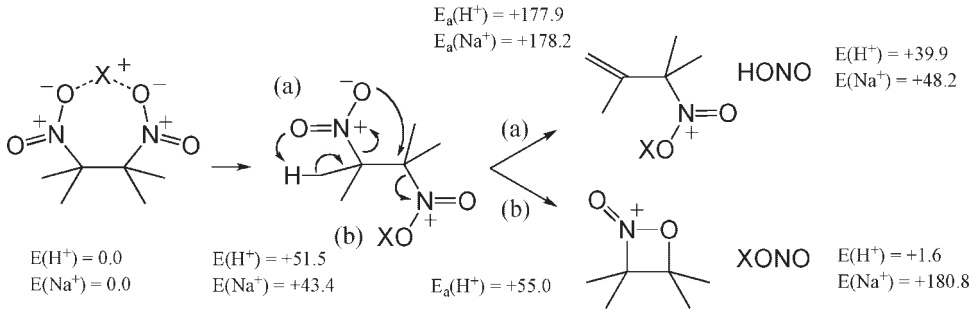

Scheme 7. Computed energetics in units of kJ mol^{-1} for two competing fragmentation pathways of $[DMNB+H]^+$ and $[DMNB+Na]^+$. Calculations conducted at the B3LYP/6-311++G(d,p) level.

in observing the $[DMNB+H]^+$ cation in both ESI and IMS experiments. Although no analogous transition state was identified for the loss of NaONO from $[DMNB+Na]^+$, the overall reaction is calculated to be endothermic by +180.8 kJ mol^{-1} with respect to the *syn*-conformer. Thus dissociation of the $[DMNB+Na]^+$ adduct via loss of either HONO (Scheme 7(a)) or NaONO (Scheme 7(b)) requires more energy than the +165.7 kJ mol^{-1} computed for dissociation of the adduct ion into a free sodium cation and neutral DMNB. The relative energetics calculated for these competing processes are consistent with the following experimental observations; (i) a much higher threshold for dissociation of $[M+Na]^+$ than of $[DMNB+H]^+$ and (cf. Fig. 5) (ii) the formation of the sodium cation (*m/z* 23) as the dominant fragmentation pathway in Fig. 5(d).

DESI-MS of DMNB

While the greater stability of metal ion adducts of DMNB in the gas phase may be difficult to exploit in the IMS detection of this taggant, these observations suggest that detection may be favoured by alternative analytical approaches such as desorption electrospray ionisation mass spectrometry (DESI-MS).[23] Figure 8(a) shows a DESI mass spectrum obtained from a hydrophobic slide spiked with DMNB obtained on a quadrupole linear ion trap mass spectrometer. The spectrum clearly indicates an abundant $[M+Na]^+$ ion from DMNB at *m/z* 199. The identity of this ion was confirmed by DESI-MS/MS (Fig. 8(b)) that reveals fragmentation congruent with that observed in the analogous ESI-MS/MS spectrum (Fig. 5(d)).

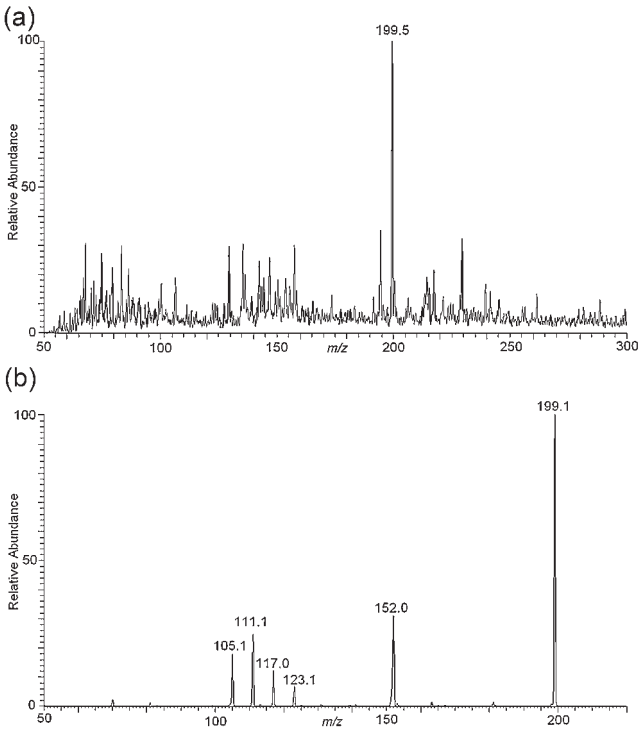

Figure 8. (a) A positive ion DESI-MS spectrum of DMNB residue deposited at ca. 50 ng cm^{-2} on a Prosolia Omni Slide™. (b) DESI-MS/MS spectrum of $[DMNB+Na]^+$ (*m/z* 199).

CONCLUSIONS

Fragmentation mechanisms have been proposed based on the tandem mass spectra of the DMNB adduct ions; $[DMNB+H]^+$, $[DMNB+Li]^+$, $[DMNB+NH_4]^+$and $[DMNB+Na]^+$. The protonated molecule was found to be susceptible to dissociation induced by heat or collision and a facile ion-molecule reaction with water was also observed on the mass spectrometric timescale. The formation of adducts with ammonium, lithium and sodium increases the precursor ion stability of ionised DMNB with respect to dissociation in ESI-MS analysis. Although the use of metal adducts may not be applicable for the detection of DMNB by conventional IMS methods, other positively charged adducts such as ammonium and nicotinamide provide viable alternatives and have previously been applied in IMS detection.[14] The propensity of DMNB to form stable sodium adducts can be exploited for the detection of the taggant from surfaces via DESI-MS.

SUPPORTING INFORMATION

Additional supporting information may be found in the online version of this article.

Acknowledgements

MRLP is supported by an Australian Postgraduate Award (Industry) and BBK is supported by an Australian Postgraduate Award. SJB acknowledges the financial support of the University of Wollongong and the Australian Research Council and the Australian Partnership for Advanced Computing (ANU, Canberra) for a generous allocation of processor time through the Merit Allocation Scheme. SE-S would like to acknowledge David Bourne (Human Protection Performance Division, Defence Science and Technology Organisation) for assistance during this work.

DOI: 10.1002/rcm

REFERENCES

1. *Convention of the Marking of Plastic Explosives for the Purpose of Detection* Report by the International Civil Aviation Organisation, 1991; Doc. 9571.
2. Danylewych-May LL, Cumming C. Explosive and Taggant Detection with Ionscan. In *Advances in Analysis and Detection of Explosives*. Kluwer Academic Publishers: Dordecht, 1993; 385.
3. Munro WA, Thomas CLP, Langford ML. *Anal. Chim. Acta* 1998; **374**: 253.
4. Perr JM, Furton KG, Almirall JR. *Proceedings of SPIE. Sensors and C3I Technologies for Homeland Security and Homeland Defence IV* 2005; 667.
5. Li X, Zeng Z, Zeng Y. *Talanta* 2007; **72**: 1581.
6. Giordano BC, Terray A, Collins GE. *Electrophoresis* 2006; **27**: 4295.
7. Germain ME, Vargo TR, Khalifah PG, Knapp MJ. *Inorg. Chem.* 2007; **46**: 4422.
8. Knapp MJ. *Fluorescent Detection of Explosives Analogs by Zn(II) Coordination Compounds*. 233rd ACS National Meeting, Chicago, IL, 2007.
9. Thomas SW III, Amara JP, Bjork RE, Swager TM. *Chem. Commun*. 2005; 4572.
10. Naddo T, Yang XM, Moore JS, Zang L. *Sensors Actuators B: Chem.* 2008; **134**: 287.
11. Wang J, Thongngamdee S, Lu D. *Electroanalysis* 2006; **18**: 971.
12. Ellis-Steinborner S, Ireland D, Provatas A, Blanksby SJ, Kirkbride P, Rivera H. Concealment Detection and Analysis Methods for MARPLEX Taggant 2,3-Dimethyl-2,3-Dinitrobutane (DMNB) *Report by the Defence Science and Technology Organisation*, 2008; DSTO-TR-2136.
13. Ewing RG, Atkinson DA, Eiceman GA, Ewing GJ. *Talanta* 2001; **54**: 515.
14. Munro WA, Thomas CLP, Langford ML. *Anal. Chim. Acta* 1998; **375**: 49.
15. Perr JM, Furton KG, Almirall JR. *J. Sep. Sci.* 2005; **28**: 177.
16. Frisch MJ, Trucks GW, Schlegel HB, Scuseria GE, Robb MA, Cheeseman JR, Montgomery JJA, Vreven T, Kudin KN, Burant JC, Millam JM, Iyengar SS, Tomasi J, Barone V, Mennucci B, Cossi M, Scalmani G, Rega N, Petersson GA, Nakatsuji H, Hada M, Ehara M, Toyota K, Fukuda R, Hasegawa J, Ishida M, Nakajima T, Honda Y, Kitao O, Nakai H, Klene M, Li X, Knox J, Hratchian HP, Cross JB, Bakken V, Adamo C, Jaramillo J, Gomperts R, Stratmann RE, Yazyev O, Austin AJ, Cammi R, Pomelli C, Ochterski JW, Ayala P, Morokuma K, Voth G, Salvador P, Dannenberg JJ, Zakrzewski VG, Dapprich S, Daniels AD, Strain MC, Farkas O, Malick DK, Rabuck AD, Raghavachari K, Foresman JB, Ortiz JV, Cui Q, Baboul AG, Clifford S, Cioslowski J, Stefanov BB, Liu G, Liashenko A, Piskorz P, Komaromi I, Martin RL, Fox DJ, Keith T, Al-Laham MA, Peng CY, Nanayakkara A, Challacombe M, Gill PMW, Johnson B, Chen W, Wong MW, Gonzalez C, Pople JA. *Gaussian03*; Gaussian Inc.: Wallingford, CT, 2004.
17. Rohner TC, Lion N, Girault HH. *Phys. Chem. Chem. Phys.* 2004; **6**: 3056.
18. McLafferty FW. *Collisionally Activated Dissociation of Low Kinetic Energy Ions in: Tandem Mass Spectrometry*. John Wiley: New York, 1983; 125.
19. Blanksby SJ, Ellison GB. *Acc. Chem. Res.* 2003; **36**: 255.
20. Ullman E. *Diazacyclobutanes* US Patent 4032519 1977.
21. Poon C, Mayer PM. *Int. J. Mass Spectrom.* 2006; **255/256**: 93.
22. Fritzsche K, Beckhaus HD, Ruchardt C. *Tetrahedron Lett.* 1988; **29**: 2805.
23. Takats Z, Wiseman JM, Cooks RG. *J. Mass Spectrom.* 2005; **40**: 1261.

DOI: 10.1002/rcm